

# A Polyimide Nanocomposite from Octa(aminophenyl)silsesquioxane

Ryo Tamaki,<sup>†</sup> Jiwon Choi, and Richard M. Laine\*

Department of Materials Science and Engineering and the Macromolecular Science and Engineering Center, University of Michigan, Ann Arbor, Michigan 48109-2136

Received August 13, 2002

Octaaminophenylsilsesquioxane (OAPS) can serve as a nanosized building block for the construction of materials with nanometer control of the periodicity of the organic and inorganic components and bonding between components. We describe here the synthesis of a prototypical three-dimensional polyimide by reaction of OAPS with pyromellitic dianhydride (PMDA). Model studies with phthalic anhydride provided useful cure conditions. Thus, stoichiometrically correct OAPS/PMDA nanocomposites were obtained following curing of NMP and DMF reaction solutions at lower temperatures and then to >350 °C/N<sub>2</sub> under vacuum. The resulting materials offer thermal stabilities in air and N<sub>2</sub> of >500 °C (5% mass loss temperature) and char yields >75%/N<sub>2</sub>. X-ray powder patterns indicate that the resulting materials are completely amorphous, as might be expected from the extreme rigidity of the organic tethers linking cube vertexes that will prevent long-range ordering from occurring during curing. These materials hold promise for high compressive strength applications.

## Introduction

Octafunctional octahedral silsesquioxanes [RSiO<sub>1.5</sub>]<sub>8</sub> (POSS) or cubic silsesquioxanes [RSiMe<sub>2</sub>OSiO<sub>1.5</sub>]<sub>8</sub> (cubes) represent three-dimensional nanobuilding blocks that offer the potential to construct a wide variety of materials nanometer by nanometer with precise control/tailoring of nanoarchitecture and properties.<sup>1–12</sup> In this

regard, we have prepared a wide variety of octafunctional cubes with polymerizable moieties that offer access to highly cross-linked (thermoset) nanocomposites with controlled porosities and high surface areas,<sup>10</sup> novel mechanical properties, and most recently potential for electronics and photonics applications.<sup>11–13</sup> POSS thermoplastic nanocomposites have also been developed that provide robust materials with a wide range of novel properties including resistance to atomic oxygen.<sup>4–8</sup>

Until recently, our efforts targeted the preparation of functionalized silsesquioxane macromonomers that thermoset to generate nanocomposites using hydrosilylation with (HSiO<sub>1.5</sub>)<sub>8</sub><sup>14</sup> or (HMe<sub>2</sub>SiOSiO<sub>1.5</sub>)<sub>8</sub> nano-platforms.<sup>14–16</sup> This approach permits the introduction of functional groups including methacrylates,<sup>2</sup> mesogens,<sup>9</sup> epoxies,<sup>3,11</sup> and alcohols.<sup>12</sup> Recently, amine-functionalized macromonomer thermosets were explored beginning with the synthesis of octa(aminopropyl)silsesquioxane, which offers access to novel amides and imides, and hints of liquid-crystalline behavior.<sup>17,18</sup>

A critical problem inherent to all of these materials is that the aliphatic components limit the thermal and mechanical properties potentials of the resulting nanocomposites. To solve these problems, we successfully

\* To whom correspondence should be addressed. E-mail: talsdad@umich.edu.

<sup>†</sup> Currently at Tyco Electronics Corporation, Technology Division, Menlo Park, CA 94025.

(1) (a) Laine, R. M.; Sanchez, C.; Giannelis, E.; Brinker, C. J., Eds. *Organic/Inorganic Hybrid Materials, Materials Research Society Symposium Proceedings*; Materials Research Society: Warrendale, PA, 1998; Vol. 519. (b) Klein, L. C.; Francis, L.; DeGuire, M. R.; Mark, J. E., Eds. *Organic/Inorganic Hybrid Materials II, Materials Research Society Symposium Proceedings*; Materials Research Society: Warrendale, PA, 1999; Vol. 576. (c) Laine, R. M.; Sanchez, C.; Giannelis, E.; Brinker, C. J., Eds. *Organic/Inorganic Hybrid Materials 2000, Materials Research Society Symposium Proceedings*; Materials Research Society: Warrendale, PA, 2000; Vol. 628. (d) Laine, R. M.; Sanchez, C.; Yang, S.; Brinker, C. J., Eds. *Organic/Inorganic Hybrid Materials, Materials Research Society Symposium Proceedings*; Materials Research Society: Warrendale, PA, 2002; Vol. 726. (e) Sanchez, C.; Soler-Illia, G. J. de A. A.; Ribot, F.; Lalot, T.; Mayer, C. R.; Cabuil, V. *Chem. Mater.* **2001**, *13*, 3061, and references therein.

(2) Sellinger, A.; Laine, R. M. *Macromolecules* **1996**, *29*, 2327.

(3) Sellinger, A.; Laine, R. M. *Chem. Mater.* **1996**, *8*, 1592.

(4) Lichtenhan, J. D.; Otonari, Y. A.; Carr, M. J. *Macromolecules* **1995**, *28*, 8435.

(5) Feher, F. J.; Budzichowski, T. A. *J. Organomet. Chem.* **1989**, *379*, 33.

(6) Feher, F. J.; Soulivong, D.; Eklud, A. G.; Wyndham, K. D. *Chem. Commun.* **1997**, 1185.

(7) Jeon, H. G.; Mather, P. T.; Haddad, T. S. *Polym. Int.* **2000**, *49*, 453.

(8) (a) Gilman, J. W.; Schlitzere, D. S.; Lichtenhan, J. D. *J. Appl. Polym. Sci.* **1996**, *60*, 591. (b) Gonzalez, R. I.; Phillips, S. H.; Hoflund, G. B. *J. Spacecr. Rockets* **2000B**, *37*, 463.

(9) Sellinger, A.; Laine, R. M.; Chu, V.; Viney, C. *J. Polym. Sci., Part A: Polym. Chem.* **1994**, *32*, 3069.

(10) Zhang, C.; Babonneau, F.; Bonhomme, C.; Laine, R. M.; Soles, C. L.; Hristov, H. A.; Yee, A. F. *J. Am. Chem. Soc.* **1998**, *120* (33), 8380.

(11) Laine, R. M.; Choi, J.; Lee, I. *Adv. Mater.* **2001**, *13*, 800.

(12) Zhang, C.; Laine, R. M. *J. Am. Chem. Soc.* **2000**, *122* (29), 6979.

(13) Laine, R. M.; Asuncion, M.; Baliat, S.; Dias Filho, N. L.; Harcup, J.; Sutorik, A. C.; Viculis, L.; Yee, A. F.; Zhang, C.; Zhu, Q. In *Organic/Inorganic Hybrid Materials*; Klein, L., De Guire, M., Lorraine, F., Mark, J., Eds.; MRS Symposium Series 576; Materials Research Society: Warrendale, PA, 1999; pp 3–14.

(14) (a) Agaskar, P. A. *Inorg. Chem.* **1991**, *30*, 2707. (b) Hasegawa, I.; Kuroda, K.; Kato, C. *Bull. Chem. Soc. Jpn.* **1986**, *59*, 2279.

(15) Hasegawa, I.; Sakka, S.; Sugahara, Y.; Kuroda, K.; Kato, C. *J. Chem. Soc., Chem. Commun.* **1989**, 208.

(16) Hasegawa, I.; Motojima, S. *J. Organomet. Chem.* **1992**, *441*, 373.

(17) Gravel, M.-C.; Zhang, C.; Dinderman, M.; Laine, R. M. *Appl. Organomet. Chem.* **1999**, *13*, 329.

(18) Feher, F. J.; Wyndham, K. D. *Chem. Commun.* **1998**, 323.

developed a route to octa(aminophenyl)silsesquioxane (OAPS), an aromatic amine (aniline) functionalized silsesquioxane free from aliphatic components.<sup>19</sup> OAPS appears to offer excellent potential as a nanoconstruction site for the synthesis of materials ranging from high-temperature nanocomposites, precursors, organic light-emitting diodes,<sup>20</sup> and multiarmed stars where the arms offer three-dimensional (3D) conductivity, to templates for high-temperature porous materials of use in catalysis, sensing, separations, and so forth.

We report here the synthesis and characterization of the first member of the OAPS imide nanocomposite family made by reaction of pyromellitic acid dianhydride (PMDA) with OAPS.

## Experimental Section

**Materials.** Reagents and solvents were used as purchased without further purification unless mentioned. OAPS was synthesized as reported previously.<sup>19</sup>

**Characterization.** *NMR Analyses.* All <sup>1</sup>H and <sup>13</sup>C NMR analyses were done in CDCl<sub>3</sub> and recorded on a Varian INOVA 400 spectrometer. <sup>1</sup>H NMR spectra were collected at 400.0 MHz using a 6000-Hz spectral width, a relaxation delay of 3.5 s, a pulse width of 38°, 30 k data points, and CHCl<sub>3</sub> (7.259 ppm) as the internal reference. <sup>13</sup>C{<sup>1</sup>H} NMR spectra were obtained at 100.6 MHz using a 25 000-Hz spectral width, a relaxation delay of 1.5 s, a pulse width of 40°, 75 k data points, and CDCl<sub>3</sub> (77.23 ppm) as the internal reference.

*Diffuse Reflectance Fourier Transform IR Spectra (DRIFTS).* DRIFTS were recorded on a Mattson Galaxy Series 3020 bench adapted with a Harrick Scientific "Praying Mantis" DR accessory (DRA-2CO), using a N<sub>2</sub> purge and KBr as a nonabsorbent medium.

*Thermal Gravimetric Analyses.* TGAs were performed on a Perkin-Elmer TGA-7 thermogravimetric analyzer (Perkin-Elmer Co., Norwalk, CT). Measurements were performed under a continuous flow of synthetic air (60 mL/min), at 10 °C/min to 1000 °C.

*GPC Analyses.* GPC analyses were performed on a Waters GPC system, using a Waters 410 RI detector and Waters 486 UV detector, Waters Styragel columns (7.8 × 300, HR 0.5, 1, 3, 4), and a PL-DCU data capture unit from Polymer Laboratory. The system was calibrated using polystyrene standards obtained from Polymer Laboratory. THF was used as the eluent, at a flow rate of 1.0 mL/min.

*X-ray Diffraction (XRD).* XRD was performed using a Rigaku Rotating Anode Goniometer (Rigaku Denki Co. Ltd., Tokyo, Japan). The working voltage and current were 49 kV and 100 mA, respectively. Cu Kα (λ = 1.54 Å) radiation with a Ni filter was used. OAPS powder was mounted and pressed on a glass holder and scanned from 2 to 40° 2θ in increments of 0.2°. OAPS/PMDA imide film was mounted on an aluminum holder and scanned following the same methods for OAPS. Bragg's law [ $d = \lambda/2 \sin \theta$ , where λ is a wavelength (0.154 nm) and θ is the Bragg angle] was used to calculate d the distance separating diffraction planes.

**Synthesis of Octa(phthalimidephenyl)silsesquioxane (OPIPS).** In a 25-mL Schlenk flask were placed OAPS (0.5 g, 0.433 mmol), phthalic anhydride (0.539 g, 3.64 mmol), and 5 mL of *N*-methylpyrrolidone. The mixture was stirred at room temperature for 5 min. The mixture was transferred into an aluminum container and heated in a furnace under nitrogen up to 130 °C at a ramp rate of 5 °C/min and kept at the temperature for 2 h. Then, the sample was heated to 350 °C at a ramp rate of 5 °C/min and kept at this temperature for 4 h. After cooling to room temperature, the mixture was dis-

solved in 10 mL of dichloromethane and precipitated into 100 mL of hexane. Yield: 0.764 g (0.348 mmol, 80.4%). <sup>1</sup>H NMR (CDCl<sub>3</sub>): 8.2–6.4 (br). <sup>13</sup>C NMR (CDCl<sub>3</sub>): 166.7, 137.0, 133.8, 131.8, 128.7, 123.5. <sup>29</sup>Si NMR (CH<sub>2</sub>Cl<sub>2</sub>, TMS, acetone-*d*<sub>6</sub>, ppm): –80.8 (br). Anal. Calcd for Si<sub>8</sub>O<sub>27</sub>C<sub>112</sub>N<sub>8</sub>H<sub>64</sub>: C, 61.3; H, 2.94; N, 5.11. Found: C, 60.0; H, 2.90; N, 5.17. Ceramic yield (in air at 1000 °C): 22.1% (calcd 21.9%). GPC *M*<sub>n</sub> 1673, *M*<sub>w</sub> 1931, PDI 1.16.

**Synthesis of Polyimide Resins from OAPS and Pyromellitic Dianhydride (PMDA).** OAPS (0.1 g, 0.0867 mmol) was dissolved in 1.9 mL of *N*-methylpyrrolidone (NMP) under nitrogen and the solution was added to an NMR (1.4 mL) solution of PMDA (0.0756 g, 0.347 mmol, 4 equiv to OAPS) at 0 °C under nitrogen while the solution was stirred with a magnetic stir bar. After 3 min of stirring at 0 °C under nitrogen, the solution was transferred to an aluminum container and was heated in a tube furnace under nitrogen. The ramp rate was 5 °C/min to 130 °C. The temperature was maintained for 2 h and raised to several curing temperatures (150, 200, 250, 300, 350, and 400 °C) with the ramp rate of 5 °C/min. The sample was cured at each temperature for 4 h and cooled to 30 °C at a ramp rate of 5 °C/min. The sample was further dried at 150 °C under vacuum for 2 h to remove the residual solvent. The sample was also prepared by the same method using *N,N*-dimethylformamide (DMF) as solvent.

## Results and Discussion

Polyimides are normally formed by reaction of diamines with carboxylic dianhydrides. The reactions proceed initially by nucleophilic attack of amine on the anhydride initially generating amic acids. This reaction proceeds at ambient temperature and, with difunctional materials, often results in soluble intermediates that can be further processed. Thereafter, much higher temperatures (>150 °C) are needed to drive condensation of the amic acid to the imide.<sup>22</sup> Optimal properties are only obtained from complete condensation; otherwise, thermal stabilities are limited by residual defects, for example, unreacted acid and amide groups. Thus, identifying appropriate curing conditions is critical.

Because OAPS is octa- rather than difunctional, even the formation of amic acid derivatives is expected to lead to materials for which complete condensation may be highly improbable. Thus, to determine the effects of curing temperature on the imidization degree and stability of the core, the phthalimide analogue was prepared as a model for the polyimide nanocomposites (Scheme 1). The phthalimide structure is essentially identical to the polyimide nanocomposite target, except that the material is expected to be soluble and therefore susceptible to standard analytical procedures. OAPS was prepared as reported previously.<sup>19</sup> The phthalimide compound was obtained by preheating a mixture of OAPS and phthalic anhydride at 130 °C for 2 h followed by postcuring at 350 °C for 4 h, all under nitrogen. These are the same reaction conditions used to prepare the polyimide nanocomposites described below. The resulting octafunctionalized compound (mp 207 °C) is soluble in common organic solvents.

<sup>1</sup>H NMR and <sup>13</sup>C NMR confirm the appearance of new aromatic groups and a carbonyl group (see Experimental Section). FTIR clearly shows symmetric and asymmetric νC=O peaks at 1786 and 1722 cm<sup>-1</sup>, respectively.

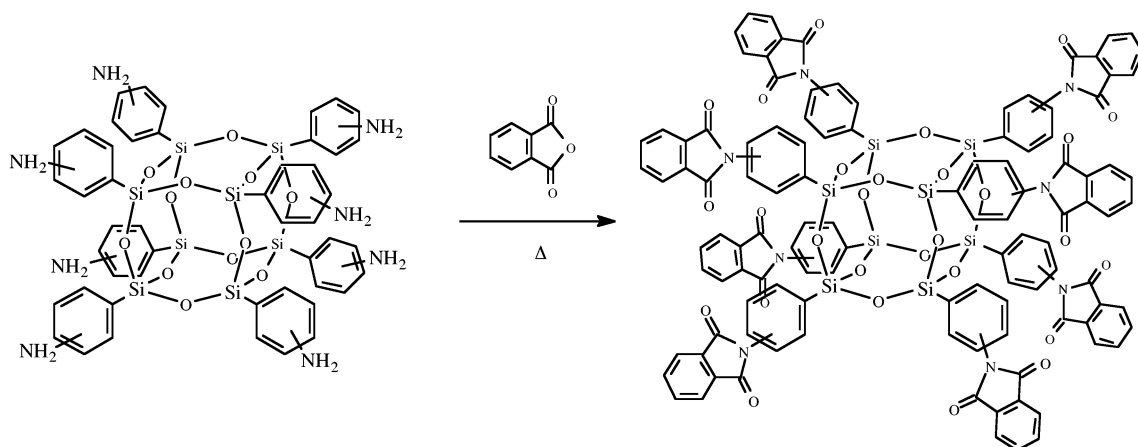
(19) Choi, J.; Harcup, J.; Yee, A. F.; Zhu, Q.; Laine, R. M. *J. Am. Chem. Soc.* **2001**, *123*, 11420.

(22) Ghosh, M. K.; Mittal, K. L. *Polyimides: fundamentals and applications*; Marcel Dekker: New York, 1996.

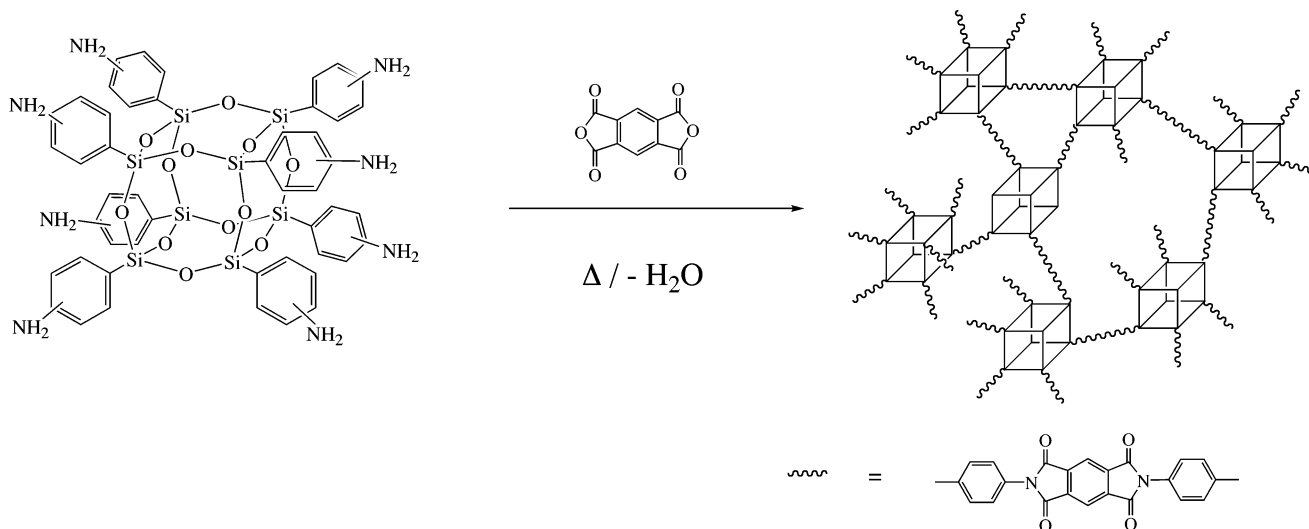
(19) Tamaki, R.; Tanaka, Y.; Asuncion, M. Z.; Choi, J.; Laine, R. M. *J. Am. Chem. Soc.* **2001**, *123*, 12416.

(20) Sellinger, A.; Laine, R. M. WO 02/05971 A1 Jan. 24, 2002.

Scheme 1



Scheme 2

Table 1. Molecular Weights of the Cubes<sup>a</sup>

cube (FW)	$M_n$	$M_w$	$M_w/M_n$
OAPS (1153.7)	1057	1133	1.072
OPIPS (2194.5)	1673	1931	1.155

<sup>a</sup> The molecular weights were obtained by GPC using polystyrene standards.

A  $\nu\text{C}-\text{N}$  peak is observed at  $1370\text{ cm}^{-1}$ . Since no original peaks from OAPS are seen in the  $^{13}\text{C}$  NMR, all of the amino phenyl groups appear to react. The TGA ceramic yield (air) was 22.1% vs 21.9% calculated, suggesting quantitative conversion to the phthalimide (OPIPS). Both the  $M_n$  and  $M_w$  obtained by GPC increase compared to those of OAPS while the polydispersity remains relatively narrow, indicating retention of the cube structure (Table 1). The fact that OAPS is substituted at multiple ring positions likely accounts for the PD seen.<sup>19</sup> The smaller than calculated GPC  $M_w$ 's likely arise because these spherical molecules exhibit hydrodynamic volumes that differ from those of the polystyrene standards used. All of these results support the effective formation of the octaphthalimide.

Theoretically, any carboxylic dianhydride can be reacted with OAPS to form polyimide nanocomposites from OAPS, as we will show in a separate paper on mechanical properties.<sup>23</sup> However, because PMDA is

very commonly used to form polyimides, it was used for our baseline studies, as suggested in Scheme 2.

Because we were concerned that attempts to melt mix the two reactants (1:2 PMDA: $\text{NH}_2$  groups) would lead to nonuniform products, we used *N*-methylpyrrolidone (NMP) as a reaction solvent. Thus, a (1:2) reaction solution was prepared at  $0\text{ }^\circ\text{C}$  and transferred to an aluminum mold and allowed to warm to room temperature. After  $\approx 5$  min at room temperature, the solution starts to gel as an amic acid network forms. The mold is then placed in a ported quartz tube and heated at  $5\text{ }^\circ\text{C}/\text{min}/\text{N}_2$  to  $130\text{ }^\circ\text{C}$ . Following a 2-h hold at  $130\text{ }^\circ\text{C}$ , the mold is again heated at  $5\text{ }^\circ\text{C}/\text{min}/\text{N}_2$  to a selected curing temperature and held for 4 h followed by cooling in the furnace. After vacuum-drying at  $150\text{ }^\circ\text{C}/2\text{ h}$ , the sample was characterized to ascertain the effects of curing temperature on extent of imidization.

The curing temperature was varied between 150 and  $400\text{ }^\circ\text{C}$  in  $50\text{ }^\circ\text{C}$  increments. Following reaction, DRIFT spectra (Figure 1) reveal the presence of symmetric and asymmetric imide  $\nu\text{C}=\text{O}$  bands at ca.  $1790$  and  $1720\text{ cm}^{-1}$ , respectively, as well as imide  $\nu\text{C}-\text{N}$  bands at  $1380\text{ cm}^{-1}$  in all samples. The anhydride  $\nu\text{C}=\text{O}$  peak at  $1890\text{ cm}^{-1}$  decreases with increases in curing temperature.

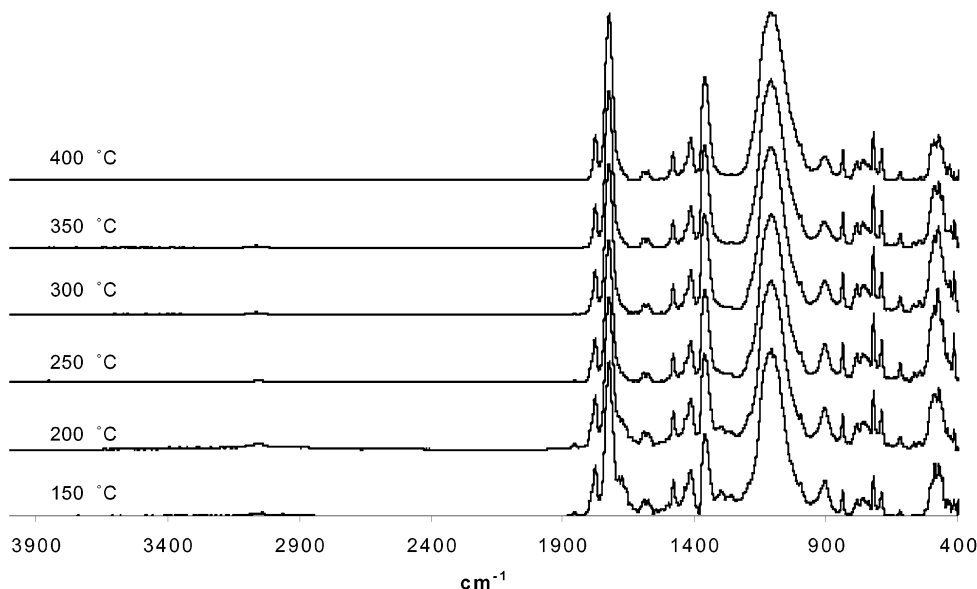


**Figure 1.** DRIFTS of polyimide composites cured to specific temperatures under  $N_2/4$  h.

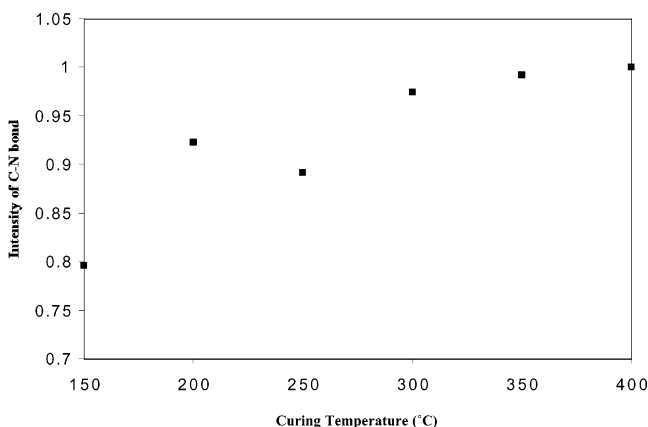


**Figure 2.** Extent of imidization vs curing temperature ( $N_2/4$  h) based on  $\nu C-N/\nu Si-O$ , error is  $\pm 10\%$ .

The cage  $\nu Si-O$  band at  $1120\text{ cm}^{-1}$  is used as an internal standard to normalize the various spectra. Since the imide  $\nu C=O$  overlaps the anhydride  $\nu C=O$ , the change in intensity of the  $\nu C-N$  peak was used to calculate the extent of imidization (Figure 2).

As shown in Figure 2, the degree of imidization increases with increases in the curing temperature. The peak intensities were normalized by dividing the intensity of each peak by the  $\nu Si-O$  intensity at  $400\text{ }^\circ\text{C}$ .

Thermogravimetric analysis was used as a second, indirect measure of curing assuming that defects (unreacted amine, anhydride, and amic acid group) will decompose before imide links. As shown in Figure 3, residues at  $1000\text{ }^\circ\text{C}$  in air, which indicate the  $SiO_2$  content in the composites, is about 26% following curing at  $250\text{--}350\text{ }^\circ\text{C}/4\text{ h}/N_2$ . This value is close to the theoretical value of 25.5 wt %. Considering the FTIR and TGA results, the extent of imidization appears to be almost quantitative at curing temperatures  $>250\text{ }^\circ\text{C}$ .

The Figure 3 data was used to calculate the degree of imidization at each curing temperature. At  $150\text{ }^\circ\text{C}$ , the degree of curing was found to be 80%, suggesting that only a slight difference in degree of imidization is obtained between 150 and  $250\text{ }^\circ\text{C}$ . However, as shown in Figure 4, the 5% mass loss temperatures, perhaps a

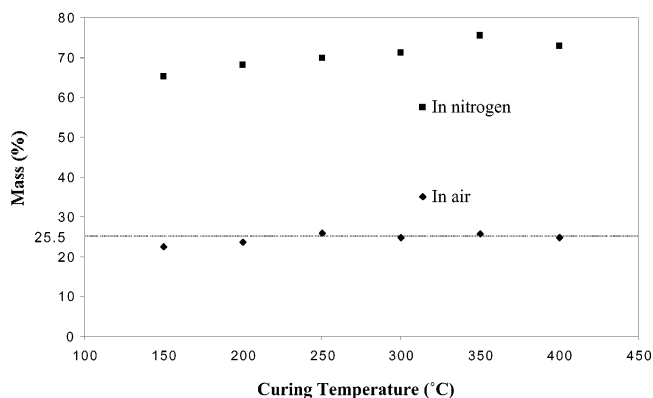


**Figure 3.** Ceramic (Char) yields at  $1000\text{ }^\circ\text{C}/\text{air} (N_2)/10\text{ }^\circ\text{C}/\text{min}$ .

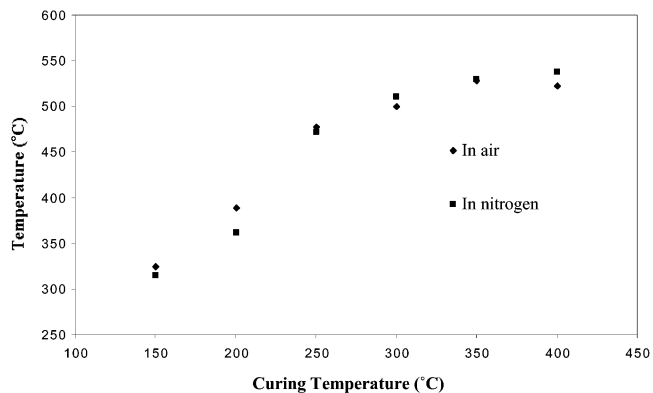


**Figure 4.** 5% mass loss temperature as a function of final curing temperature.

better measure of defect densities, are strongly affected by curing temperature. The product obtained after curing at  $150\text{ }^\circ\text{C}$  has a 5% mass loss at  $325\text{ }^\circ\text{C}$ , both in air and  $N_2$ , whereas the sample cured at  $350\text{ }^\circ\text{C}$  has a 5% mass loss at  $530\text{ }^\circ\text{C}$  in air and  $540\text{ }^\circ\text{C}$  in  $N_2$ . Char yields at  $1000\text{ }^\circ\text{C}$  also increase with increases in curing temperature to a maximum of 75 wt % (Figure 3).

When DMF is used as the solvent, the resulting thermal stabilities are lower, suggesting less imidization, giving 5% mass loss in air and  $N_2$  of 505 and 500

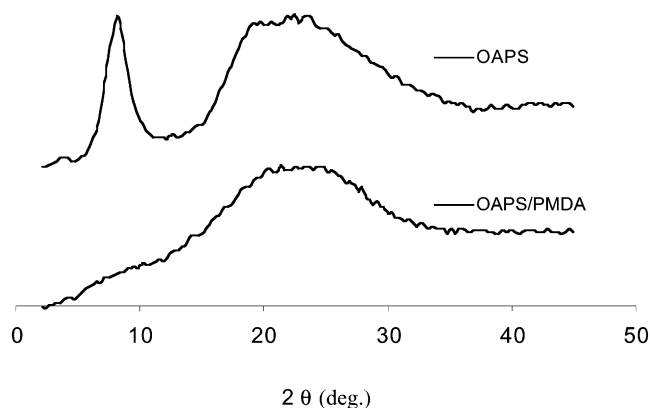


**Figure 5.** XRD before and after the reaction with PMDA.

°C, respectively, for samples cured at 350 °C. NMP has a higher boiling temperature than DMF and probably stays in the gel longer, thereby reducing viscosities and aiding diffusion of reactants.<sup>22</sup>

Powder X-ray diffraction (XRD) studies of OAPS shows a peak at 8°  $2\theta$  that corresponds to a  $d$  spacing of 1 nm (Figure 5). This diffraction peak can be explained by some long-range order in solid OAPS.<sup>23,24</sup> The broadness of the peak can be attributed to the presence of substitutional isomers.<sup>19</sup> The broad halo at ~20°  $2\theta$  may be associated with Si–O–Si linkages.<sup>25,26</sup> The XRD pattern after imidization at 350 °C is that of a completely amorphous material, which is not surprising given that imidization should create a very rigid network with very high viscosity that cannot be ex-

pected to develop long-range order. In contrast, replacing PMDA with oxydiphthalic anhydride (ODA) does provide sufficient flexibility to observe some ordering in OAPS/ODA nanocomposites, as we will discuss in a future paper.<sup>23</sup>

If, as our observations suggest, a high degree of imidization is obtained, then one might expect that the high rigidity and linearity of the imide tether between cubes should create nanoporosity. However, none could be detected by porosimetry, although multiple efforts were made. The high thermal stability of these materials is not unexpected given what is known about purely organic polyimides. However, what is novel here is that these materials cure almost completely to give a three-dimensional polyimide. Such materials can be expected to offer good-to-excellent compressive strength, a property lacking in linear polyimide materials, especially fibers. In addition, although it has not been measured, the coefficient of thermal expansion of these materials should be lower than linear polyimides, suggesting utility for electronic substrates. In a future paper, we will discuss the mechanical properties of OAPS/ODA nanocomposite materials.<sup>23</sup>

**Acknowledgment.** We would like to thank FAA for their initial support of this work through Grant No. 95-G-026. This work was also supported in part by the U.S. Air Force through a contract with Edwards AFB. We would also like to thank Warner-Lambert for partial support of this work. We would like to thank Clariant Corp. for a gift of  $\text{PhSiCl}_3$ .

(24) (a) Barry, A. J.; Daudt, W. H.; Domicone, J. J.; Gilkey, J. W. *J. Am. Chem. Soc.* **1955**, *77*, 4248. (b) Brown, J. F., Jr.; Vogt, L. H., Jr.; Prescott, P. I. *J. Am. Chem. Soc.* **1964**, *86*, 1120.

(25) Andrianov, A. A.; Zhdnov, A. A.; Levin, V. Y. *Annu. Rev. Mater. Sci.* **1978**, *8*, 313.

(26) Zheng, L.; Waddon, A. J.; Farris, R. J.; Coughlin, E. B. *Macromolecules* **2002**, *35*, 2375.

**Supporting Information Available:** Figures of  $^1\text{H}$  NMR,  $^{13}\text{C}$  NMR, and FT IR spectra of OPIPS (PDF). This material is available free of charge via the Internet at <http://pubs.acs.org>. CM020797O